Chapter 2

Amphiphilic Ionic Perylenediimides: Structures, Self-Assembly Studies and Biomedical Applications

Meizhen Yin and Baozhong Lü

Additional information is available at the end of the chapter

http://dx.doi.org/10.5772/intechopen.68399

Abstract

Amphiphilic ionic perylenediimides (AIPDIs) with well-defined structures have been widely studied, which involve abundant non-covalent interactions. Among these interactions, electrostatic interactions serve as the primary force that may be followed by other non-covalent interactions like π–π stacking. Taking advantage of these tunable interactions between simple AIPDI-building blocks, AIPDIs are widely used for constructing increasingly complex structures at varying scales. Besides, AIPDIs with outstanding photochemical stability exhibit high fluorescence quantum yields (FQYs) in aqueous solution, because hydrophilic substituents of AIPDIs can shield the inner perylene chromophores and weaken π–π stacking, contributing to the improvement of water solubility and the suppression of aggregation-caused quenching (ACQ). AIPDIs with excellent water solubility, strong FQYs and desired interactions with charged components in cells and tissues hold great promise for various biomedical applications, which can be concluded in three hierarchical levels, which is *in vitro,* live cell and tissue.

Keywords: amphiphilic ionic perylenediimides, fluorescence, self-assembly, biomedical applications

1. Introduction

Amphiphilic ionic self-assembly (AIS) is an important method to construct complex nanostructures by using non-covalent interactions of simple ionic molecular building blocks. Because of the well-defined structures, amphiphilic ionic molecules (AIMs) are studied widely in the field of AIS. Various nanostructures are obtained by the self-assembly of AIMs and the relationship between the morphologies and parameters was discovered by theoretical studies [1–8]. AIMs are designed and fabricated to form various nanostructures such as helical

fibres, nanotubes, nanospheres and so on [9–12]. Among these works, Zhang and Eisenberg studied the effects of hydrophobic/hydrophilic ratio, chemical structure, temperature, concentration and solvent on the self-assembly behaviours of AIMs [13]. AIMs self-assemblies endow AIMs with enhanced stabilities, improved water solubility and increased fluorescence intensity, making them promising candidates in biomedical applications [10, 14–21]. As an attractive chromophore, perylene-3,4,9,10-tetracarboxylic acid diimides (PDIs) have been generally used in organic electronic and photovoltaic fields for their broad absorption range, high extinction coefficients, high fluorescence quantum yields (FQYs) as well as outstanding stability. In particular, amphiphilic ionic perylenediimides (AIPDIs) are found to form tunable supramolecular-ordering constructions by a well-known non-covalent force, that is, electrostatic interaction, which is operative in AIS. This electrophorus supramolecular process was firstly introduced by Faul and Antonietti [22], who found water-soluble molecular building blocks self-assembled with oppositely charged surfactants by electrostatic interactions as the primary force. This self-assembly approach has been successfully applied to AIPDIs for their hierarchical organization in aqueous solution and bulk solid state as well. AIPDIs exhibit good water solubility, strong fluorescence and desired interactions with charged components in cells and tissues. Moreover, AIPDIs emit fluorescence above 500 nm, which effectively avoid the interference of the autofluorescence from organism. All the advantages of AIPDIs make them excellent candidates for biomedical materials. In this chapter, we describe self-assembly behaviours of AIPDIs and focus on their chemical structures, self-assembly studies and biological applications.

2. Structures and self-assemblies of AIPDIs

In general, AIPDIs are synthesized by the modification with ionic substituents in the bay region, ortho or imide positions of PDIs (**Figure 1A**). The modifications in the imide positions of PDIs with ionic substituents will improve solubility and minimally affect the optical properties. By contrast, substituents in the bay region will lead to a twist of perylene core and changes in optical properties such as significant bathochromic shift. These modification strategies of

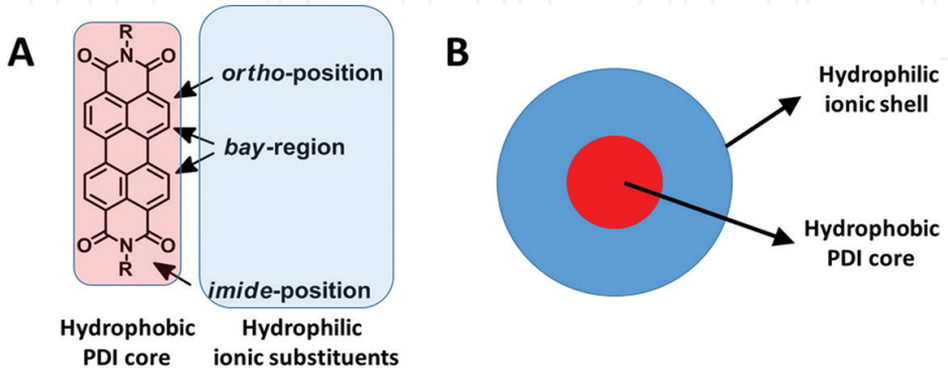

Figure 1. (A) General structure and hydrophobicity-hydrophilicity of AIPDIs, (B) schematic diagram of AIPDI core-shell structure.

PDIs in the imide position and bay region have attracted great interests in self-assembly behaviours because various intermolecular forces are introduced in this way. Besides, it will affect electronic and optical properties but not contort the two naphthalenes when selectively functionalized in the ortho positions of PDIs.

The fluorescence intensity and water solubility of modified PDIs are significantly improved compared with the unsubstituted PDIs [23]. Typically, the charged substituents can serve as the shell of PDI core, resulting in core-shell structure of AIPDIs (**Figure 1B**). In addition, the ionic substituents could provide electrostatic forces between the PDI molecules themselves or other charged guests. Intermolecular π-π stacking of PDIs could be attenuated by steric hindrance and electrostatic repulsion forces, leading to good water solubility and strong fluorescence of dye molecules.

2.1. Self-assembly of anionic AIPDIs

The self-assembly of AIPDI without surfactants was first studied by Ford in the 1980s [24]. In this fundamental research, concentration-dependent UV/vis absorption and fluorescence spectroscopy were studied. It showed that the anionic di(glycyl) PDI derivative **1a** (**Figure 2**) existed in an equilibrium between monomer and dimer of **1a** in alkaline aqueous solution with an association constant of $K = 1.0 \times 10^7\ M^{-1}$ at 24°C. The absorption maximum of dimers of this core unsubstituted dianionic AIPDI was strongly hypochromatic shift (32 nm) with considerable band broadening as compared with that for the monomer (λ_{max} = 532 nm, at $c = 8.7 \times 10^{-9}$ M), which was illuminated by molecular excitonic theory for parallel-oriented sandwich-type dimer. The fluorescence of the dimers was drastically quenched with a quantum yield of $\Phi_F < 0.02$ as compared with that of monomeric PDI anion. More interestingly, they found a considerable salt (NaCl) effect on the aggregation of dianionic AIPDI **1a**, which was discussed in light of counterion shielding of the electrostatic repulsion between the negatively charged AIPDI molecules. Although the synthesis and optical characterization of higher homologues of dicarboxylate **1a** with longer alkyl chains (**1b–d**) were reported already in the 1990s, their self-assembly behaviour has not been explored until today [25].

Malik and co-workers reported a pair of chiral AIPDIs **2** (**Figure 3**) modified with aspartic acid (L or D) [26]. The reddish-brown hydrogel with reddish fluorescence formed when the pH of **2** of aqueous solution decreased to 4. Atomic force microscopy (AFM) images revealed that dried

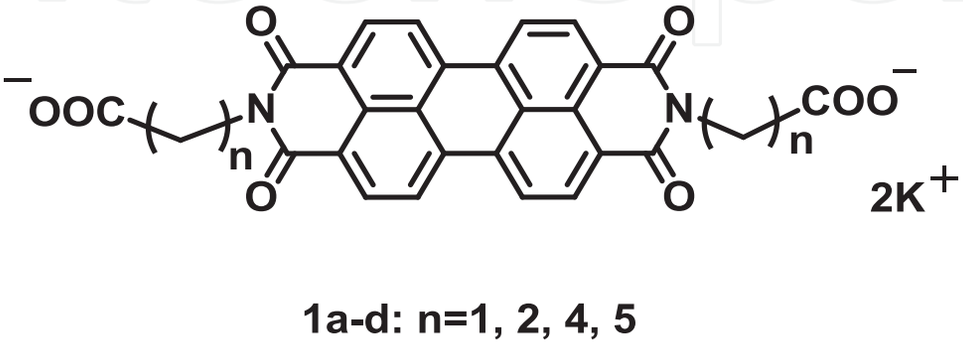

1a-d: n=1, 2, 4, 5

Figure 2. Anionic AIDPIs of **1a–d**.

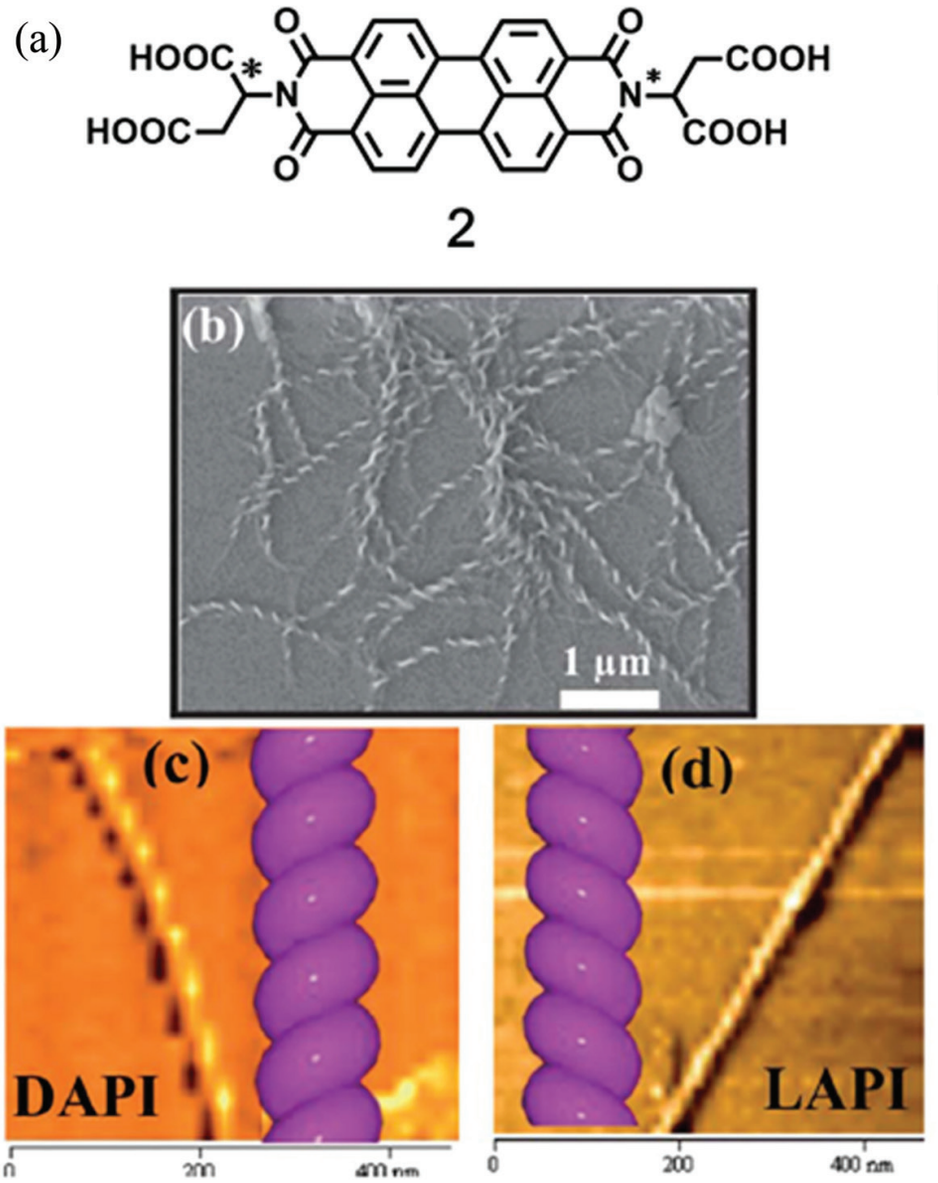

Figure 3. (a) Molecular structure of modified AIPDI **2**. (b) FE-SEM image of a **D-2**-dried gel. (c) AFM image of **D-2** gel and (d) **L-2** gel prepared on a mica substrate. Copyright (2013) The Royal Society of Chemistry.

L-2 or **D-2** gel formed helical fibres with a diameter of 20 nm and a pitch length of 20 nm. The perylene core played an important role during the formation of helical thick filaments. Further studies showed that the synergistic effect of π–π stacking, intermolecular hydrogen and chiral effect guided the aggregation and gelation in water during the decrease of pH.

2.2. Self-assembly of cationic AIPDIs

The synthesis and optical properties of AIPDIs **3a,b** modified with cationic ammonium side chains were reported already in the mid-1990s (**Figure 4**) [25, 27]. Subsequently, the self-assembly behaviour of AIPDIs **3a,b** has been reported. Trimethyl ammonium ethylene-functionalized dicationic AIPDI **3a** with iodide counterions has been studied by many

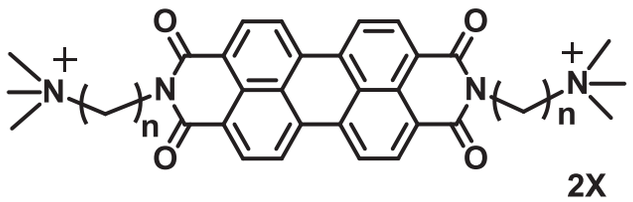

3a: n=2 X=I⁻
3b: n=3 X=I⁻

Figure 4. Cationic AIPDIs **3**.

research groups with different objectives. Wei and co-workers first studied the self-assembly of AIPDI **3a** in the solvent of water and methanol [28]. They found that this cationic AIPDI **3a** could self-assemble into nanotubes with diameters of ca. 100–300 nm in aqueous medium, while long nanorods with diameters of ca. 200–300 nm were formed from methanol solution as verified by scanning electron microscopy (SEM) and transmission electron microscopy (TEM) (**Figure 5**). Then, Faul and co-workers reported the formation of supramolecular polymers by ionic self-assembly of the same cationic AIPDI **3a** with anionic copper-phthalocyanine tetrasulphonate in water. These supramolecular polymers are fibre-like structure as observed by different imaging techniques [29]. Very recently, this research group reported the self-assembly behaviours of a chiral derivative of **3a** containing a benzyl substituent at the chirality centre adjacent to the ammonium group. Their detailed studies showed that the self-assembly of this inherently chiral cationic AIPDI in water can be described according to the isodesmic model, and the molecular chirality of the imide side chains is transmitted to the self-assembled supramolecular structures due to induced CD effects that were observed [30]. AIPDI **3a** could also self-assemble together with other guests. Negatively charged tetrasulphonated zinc-porphyrin self-assembled with the AIPDI **3a** in water, resulting in a host-guest supramolecular assembly that showed photoinduced electron-transport property [31]. Hydrogel formed by co-assembling of this cationic AIPDI **3a** with a bicarboxylate functionalized oligo(phenylenevinylene) derivative [32]. Furthermore, layer-by-layer (LbL) deposition was used to proceed electrostatic self-assembly of this positively charged AIPDI **3a** together with two other derivatives. The deposited thin films incorporating less than 15 bilayers are composed of serpentine nanofibres as revealed by AFM [33]. Moreover, many complexes formed by self-assembly of ionic AIPDI **3a** with different negatively charged surfactants have thermotropic and lyotropic liquid crystalline (LC) properties. Trimethyl ammonium propylene-functionalized AIPDI **3b**, a higher homologue of **3a**, was reported to self-assemble with negatively charged adenosine triphosphate (ATP). Chiral superstructures with a right-handed helical stack of AIPDI **3b** formed via electrostatic forces and π–π interactions [34].

Yao and co-workers [35] synthesized a PID derivative with pyridyl in the bay region. They found that the self-assembly of amphiphilic AIPDI **4** (**Figure 6**) can be subtly controlled by tuning the environmental parameters. Mono-protonated dye **5** and doubly protonated dye **6** evoke new intermolecular interactions in the bay regions. These new secondary forces typically influence π-π stacking, thus leading to new aggregations. In particular, the ratio of

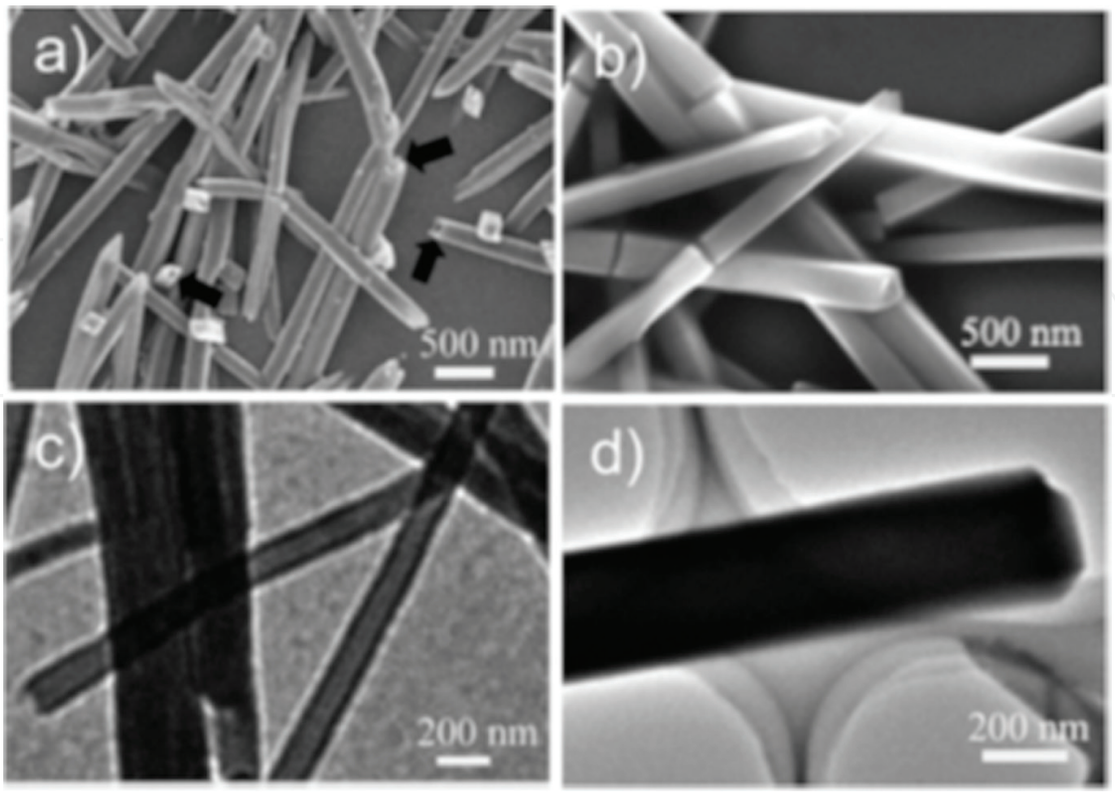

Figure 5. SEM (a, b) and TEM (c, d) images of nanotubes (a, c) and nanorods (b, d) formed from aqueous and methanol solutions (0.3 mM) of AIPDI **3a**, respectively. Copyright (2009) American Chemical Society.

hydrochloric acid (HCl)/methanol/water was utilized to adjust the solvent environment and self-assembly parameters, and then five different phases formed by subtle AIS (**Figure 7**). In this way, the representative self-assembled nanostructures were nanoparticles, nanotapes and corresponding one-dimensional (1D) aggregations, nanoplates, hollow nanospheres and corresponding 1D aggregations. As the most important factor, the water fraction (Rw)

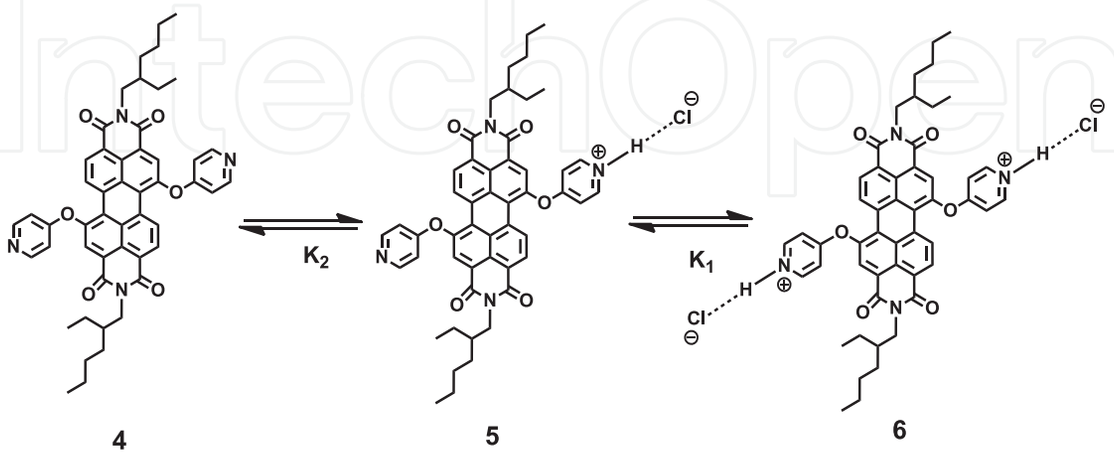

Figure 6. Dynamic protonation among dyes **4**–**6**.

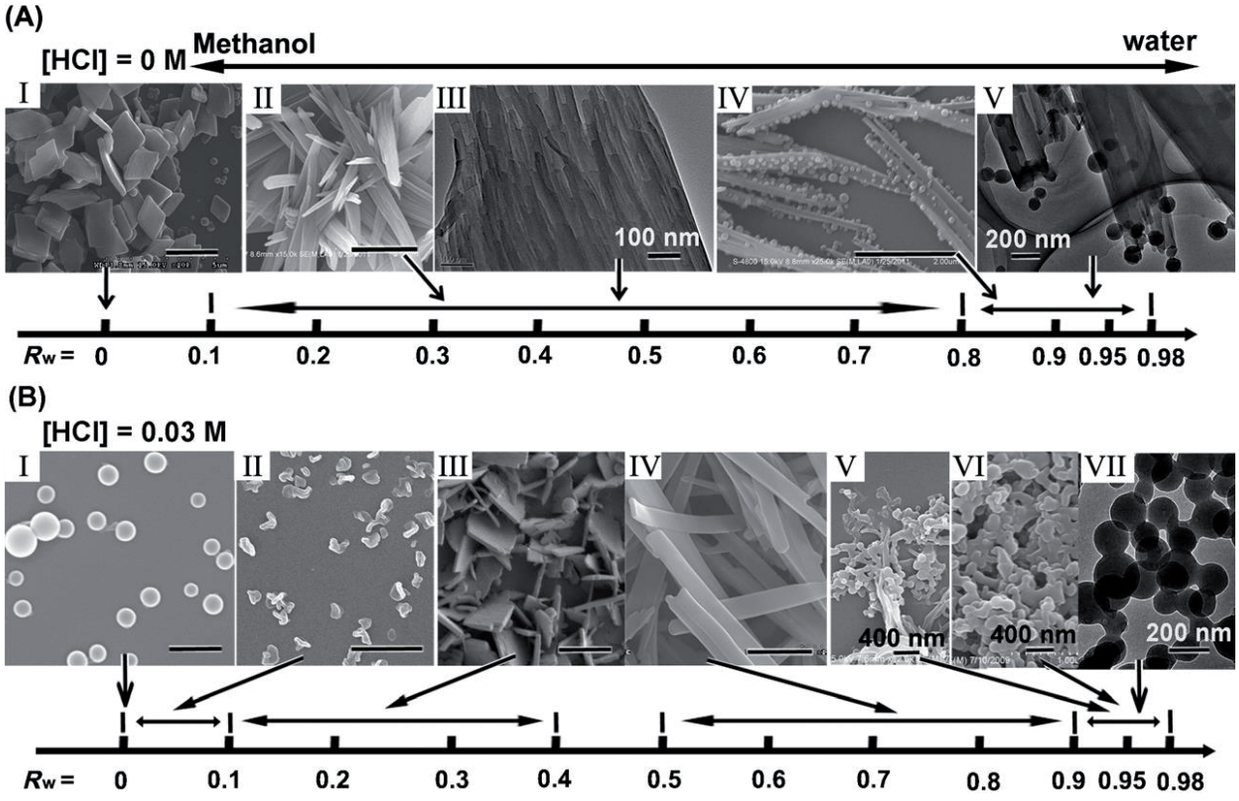

Figure 7. The typically 1D phase diagram and morphologies formed either from (A) chromophore **4** or (B) chromophore **6** equilibrating with dyes **5** and **4** at [HCl] = 0.03 M controlled by Rw. A-III, A-V and B-VII are TEM images. [dye] = 1×10^{-3}M is constant. The scale bar is 2 mm in the unlabelled pictures. Copyright (2012) John Wiley and Sons.

and the concentration of hydrochloric acid [HCl] play the crucial role to form the specific nanostructures. For example, nanotapes formed at low [HCl] and Rw values, whereas hollow nanospheres were observed when either the Rw is low or [HCl] is high, or both. To summarize, this work provides a phase diagram by tuning Rw and [HCl] as two variables. Such a self-assembly phase diagram summarizes the fine control on the self-assembled nanostructures, and inspires us to regulate the self-assembly of AIPDI by simply tuning the parameters.

2.3. Self-assembly of AIPDIs in charged surface

The attachment of charged dendritic substituents at the imide positions or in the bay regions of PDI can effectively suppress the aggregation of perylene chromophores and provide hydrophilia. The ionic nature of these dendrimers can self-assemble on the charged surface of gold or alumina template. Yin, Müllen et al. firstly reported a series of core-shell structures, by using shape-persistent polyphenylene dendrimer as a scaffold and a stabilizer. The outer flexible polymer shells contributed to proton-conducting property [36, 37]. Thus, a core-shell architecture **7** containing phosphonic acids was synthesized and its self-assembly on a modified gold substrate via electrostatic interaction was studied. AFM in **Figure 8** shows many uniformly dispersed globular particles, demonstrating unimolecular polymeric micelles [38].

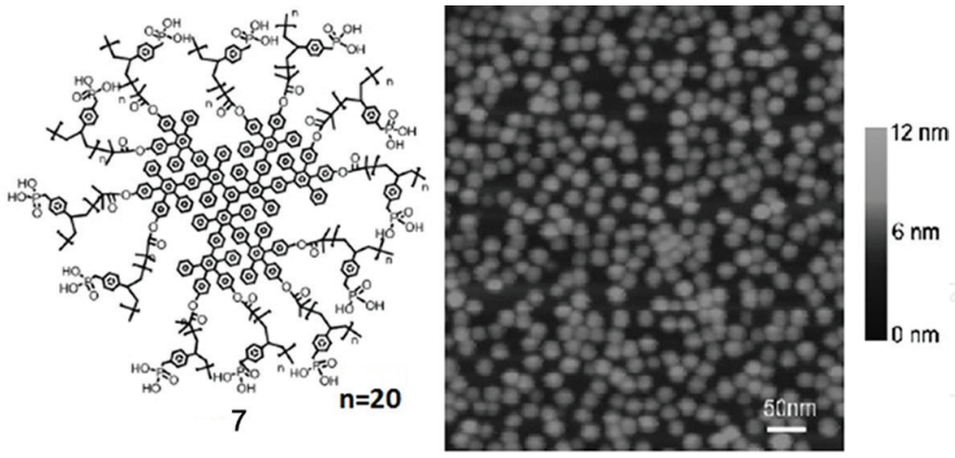

Figure 8. Core-shell structure **7** and AFM image of self-assembled unimolecular polymeric micelles of **7** on a modified gold film. Copyright (2012) John Wiley and Sons.

Recently, Yin, Müllen et al. reported a series of fluorescent core-shell AIPDI macromolecules based on polyphenylene dendrimers [39–41]. In order to introduce ionic functionalities such as amine and carboxylic acid, flexible polymer shell was attached to the shape-persistent cores. As representatives, core-shell AIPDIs **8c** and **9b** with opposite charges were synthesized (**Figure 9**) [42, 43]. AIPDIs **8c** and **9b** have a fluorescent PDI core attached with polyphenylene dendrimer and a flexible cationic or anionic polyelectrolytes shell, which contributes to the water solubility and pH sensitivity. Because of the polyelectrolyte nature, AIPDIs **8c** and **9b** could form pH-responsive globular unimolecular polymeric micelles in aqueous solution, which was confirmed by small-angle X-ray scattering (SAXS) [42]. The authors attributed the pH-responsive behaviour of AIPDIs **8c** and **9b** to the ionization or deionization of the star polyelectrolytes, which leads to the variation of volume phase and optical properties.

Templated self-assembly of the oppositely charged polymers was also investigated. LbL deposition of oppositely charged **8b** and **9a** in a porous alumina template was used to fabricate multilayer films. Due to the electrostatic interactions between charged **8b** and **9a** and alumina membrane, **8b** and **9a** assembled on the alumina surface during the LbL process. **Figure 10A** shows TEM image of self-assembled hollow nanotube after the removal of the

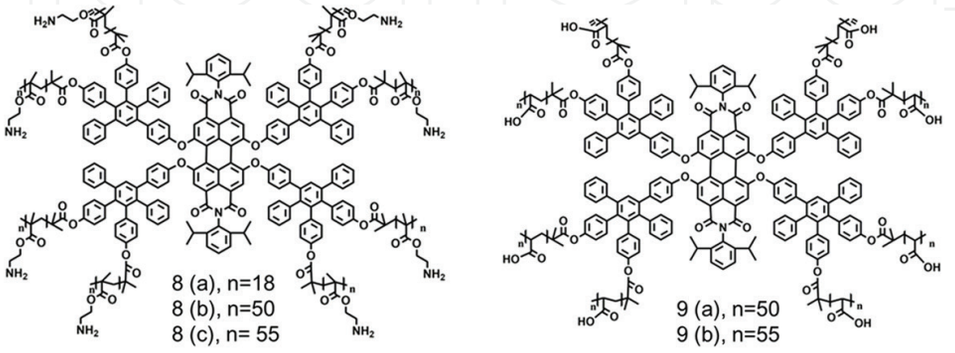

Figure 9. Core-shell of AIPDI macromolecules **8** and **9**.

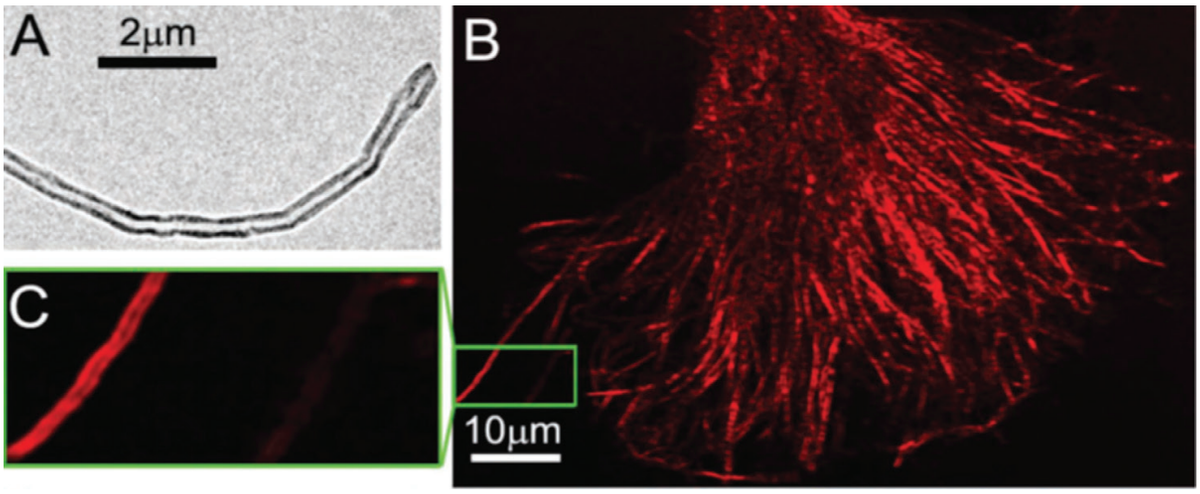

Figure 10. Self-assembled nanotubes fabricated by LbL deposition of AIPDI **8** and **9**. (A) TEM and (B, C) corresponding fluorescence microscope images of self-assembled nanotubes. Copyright (2011) John Wiley and Sons.

alumina template. Large-scale fluorescent nanotubes in solution were presented with a fluorescence microscope as shown in **Figure 10B** [43].

3. Biological applications of AIPDIs

Charged components are widely existed in organism, such as the negatively charged extracellular matrixes (ECMs), membranes, DNA and positively charged histone proteins. Therefore, water-soluble AIPDIs with charges on the surface would interact with the charged biological components through electrostatic forces. Moreover, AIPDIs have good water solubility and strong fluorescence, the fluorescence and absorption maxima of AIPDIs are above 500 nm, which could minimize the background noise from organism auto-fluorescence. All the advantages make them excellent candidates for biomedical materials. The biological applications of water-soluble AIPDIs are summarized below including imaging studies of living cells and tissues.

3.1. *In vitro* studies

Because of the fluorescence nature, the cationic AIPDIs were widely studied in the field of molecular detection in organism. As mentioned above, interactions between AIPDI and biological molecules are the most important part for researches in cells and tissues. Yin et al. have reported a type of fluorescent nanotubes fabricated by oppositely charged **10** and **11** which could serve as DNA biosensors (**Figure 11**) [43]. As shown in **Figure 12A**, positively charged AIPDI **10** on the outer surface of the nanotubes can interact with DNA by electrostatic forces. The complex of self-assembled nanotube and DNA showed obviously improved fluorescence intensity when compared with original nanotube because of the protection of PDI chromophore in aqueous solution. Subsequently, Yin et al. reported an ultrasensitive and selective DNA sensor by using the negatively charged AIPDI **12** as a donor and DNA targets labelled

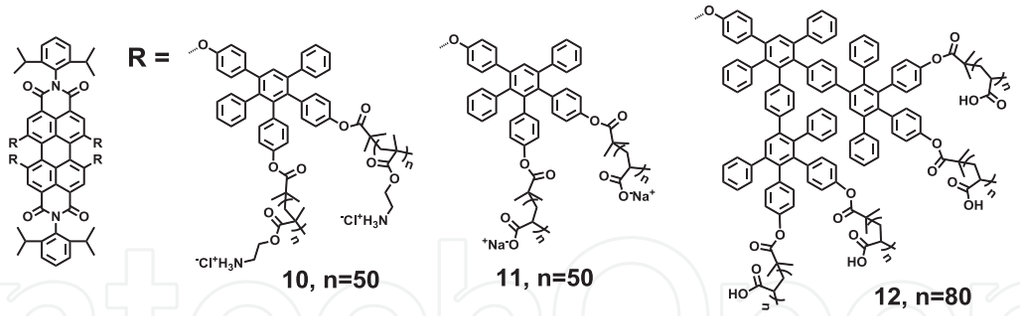

Figure 11. Chemical structures of AIPDIs **10–12**.

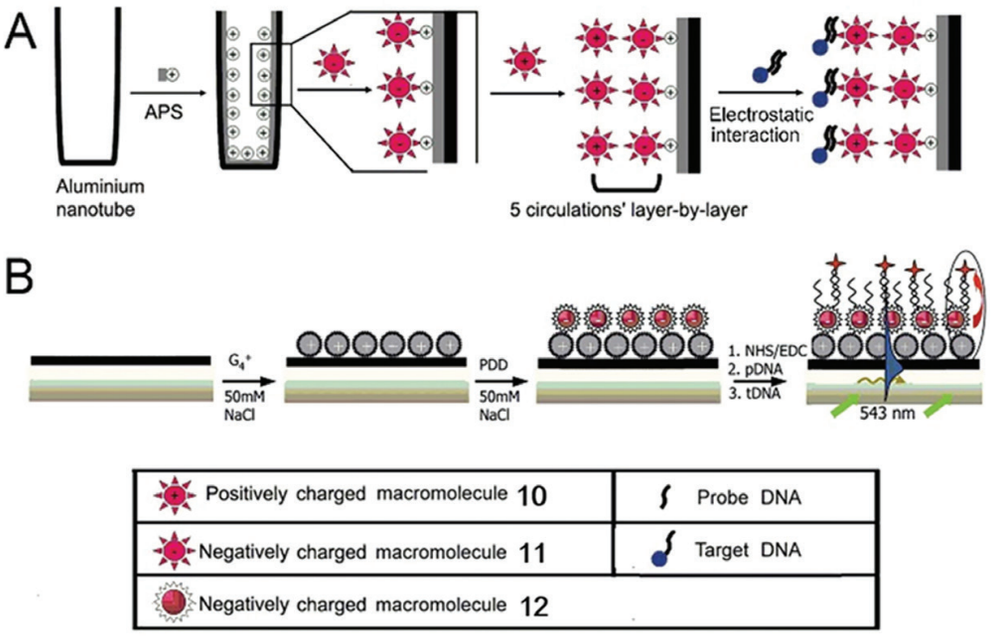

Figure 12. (A) Formation of fluorescent nanotubes by LbL deposition of **11** and **10**. Copyright 2011, John Wiley and Sons. (B) Energy transfer process between AIPDI **12** and Cy5. Copyright 2011, John Wiley and Sons.

by Cy5 as an acceptor (**Figure 12B**). Excitation energy was transferred from Cy5 to AIPDI **12** upon excitation at 543 nm. Due to energy transfer (ET), the sensor is ultrasensitive, selective and time-resolved (**Figure 12B**) [44].

Based on the interaction between probe **13** and nucleic acid aptamer, a fluorescent molecule **13** with switching properties is reported and used for sensitive and selective detection of proteins (**Figure 13**) [45]. In aqueous solution, probe **13** exists in monomeric forms, thus strong fluorescence can be observed (**Figure 13-1**). Nucleic acid aptamer is negatively charged, thus strong electrostatic interactions occur between AIPDI **13** and aptamer, leading to the aggregate formation. Due to the aggregation-caused quenching (ACQ) effect, the fluorescence intensity of the solution significantly decreases (**Figure 13-2**). Lysozyme has higher affinity to aptamer than that of **13**. As a result, aggregated **13** is replaced by the lysozyme and the intensity of fluorescence signal of **13** will be restored since **13** becomes monomeric state (**Figure 13-3**).

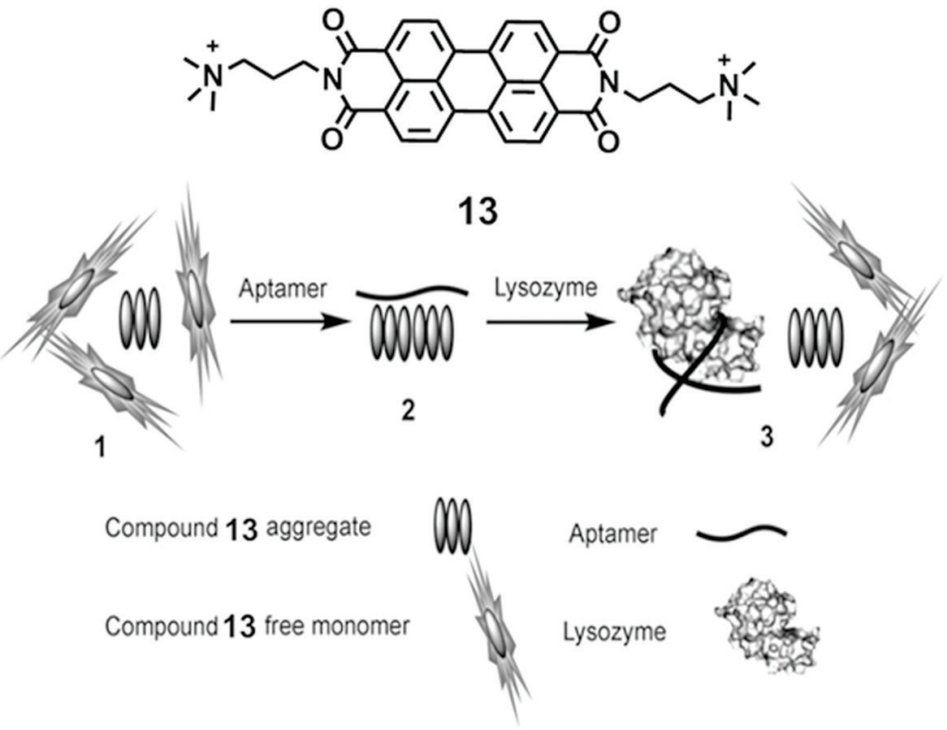

Figure 13. Chemical structures of cationic AIPDI **13** and schematic illustration for selective detection of lysozyme. Copyright (2010), John Wiley and Sons.

3.2. Live cell studies

With good selectivity and sensitivity, fluorescence bioimaging offers microscopic visualization of the organism. Thus, water-soluble AIPDIs with high fluorescence intensity have attracted great attention in bioimaging.

Yin et al. reported that dendritic AIPDIs **14a–c** and star-shaped polymers **15–16** are great gene delivery and bioimaging agents (**Figure 14**) [46, 47]. The fluorescence microscopy images indicate that all the cationic AIPDIs are internalized into cells and the cell viabilities of **14a–c**, **15** and **16** are all above 90%, suggesting that the AIPDIs have low cytotoxicity. All these AIPDIs molecules, **14a–c**, **15** and **16,** can serve as DNA delivery agents and can form probe/DNA complexes via electrostatic interaction with negatively charged DNA. The fluorescence images of **14c**/DNA and **16**/DNA complexes (**Figure 15**) showed that **14c** (A–A″) and **16** (B–B″) could deliver DNA into cells. Notably, the gene transfection efficiency of **14a–c** has an increased tendency with the increased generation of the dendritic molecules due to more positive charges and the larger external branches of dendritic molecules.

3.3. Tissue imaging

Fluorescence labelling, the process of attaching a reactive probe to a functional group of target molecule with covalent or non-covalent interactions, is usually used for tissue imaging. Generally, the target structure, such as antibodies, proteins, amino acids and peptides, is charged. Thus, based on the electrostatic interactions with those charged electrolytes, AIPDIs have unique advantages in tissue imaging.

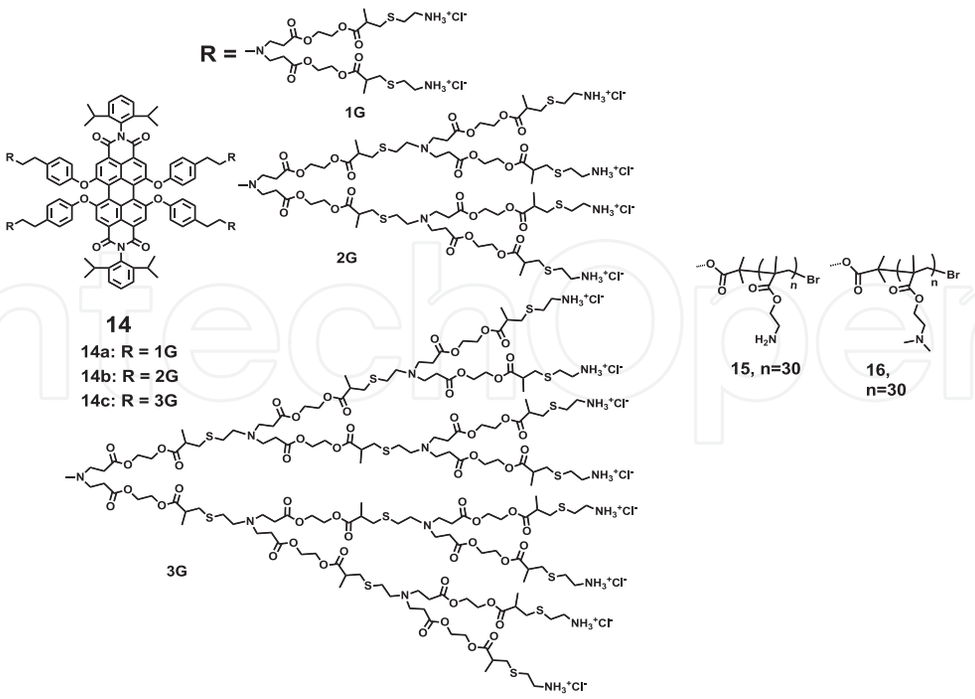

Figure 14. Chemical structures of macromolecules **14–16**.

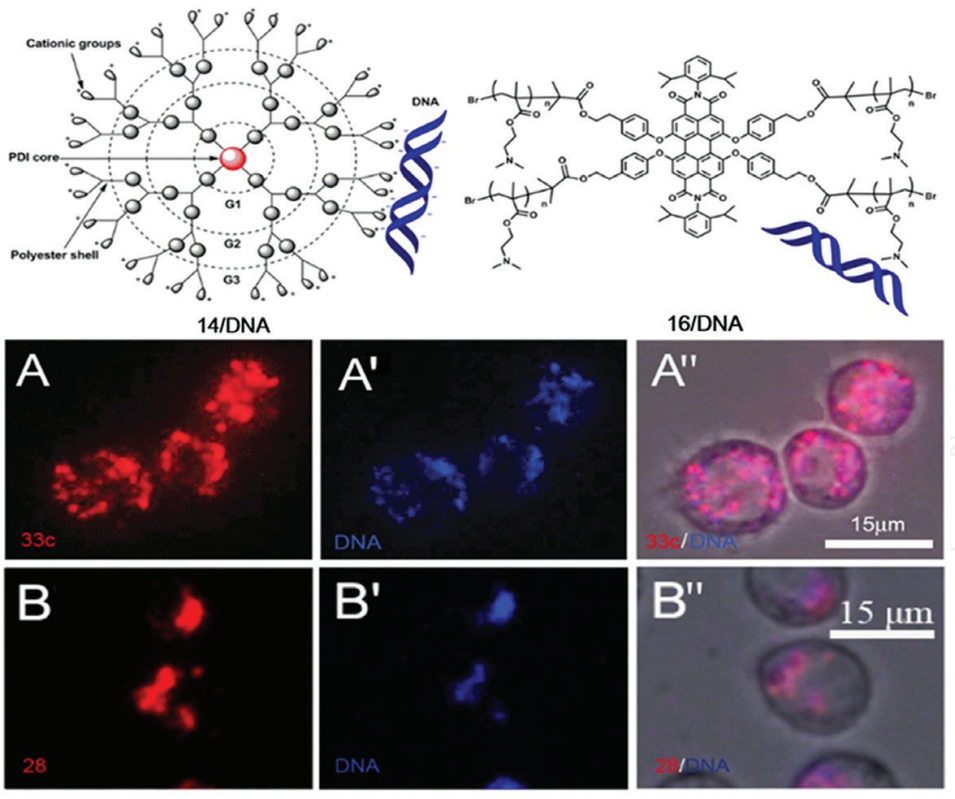

Figure 15. Schematic illustration of the complexes formed by **14c** or **16** and DNA. Fluorescence images of the **14c** (A) and **16** (B) internalizing into cells; A′ and B′ are fluorescence images of DNA labelled by CXR Reference Dye; A″ and B″ are images of the complex of **14c**/DNA and **16**/DNA. Copyright (2013), Royal Society of Chemistry for Ref. [47] and copyright (2014), American Chemical Society for Ref. [46].

The star polymer **17** with negative charges cannot enter the living cells [48], but can specifically label cell nucleus in fixed tissues via binding to positively charged nuclear proteins [49]. As shown in **Figure 16**, the red staining of AIPDI **17** shows almost no overlap with the membrane marker CD8-GF (green part, **Figure 16A**), or cytoskeletal marker anti-α-tubulin antibodies (green, **Figure 16B**). In **Figure 16C** and **D**, the staining of AIPDI **17** has the same pattern with DAPI (commercial DNA dye, blue, **Figure 16C″**) and demonstrates a prominently co-localization effect with histone H4 (green, **Figure 16D″**AIPDI **17**, bearing multiple carboxyl groups, could specifically bind positively charged histone, leading to specific labelling of cell nucleus. This work provides a fascinating substitute for conventional costly antibodies or chromophores with broad emission such as commercial dye, DAPI.

By contrast, the positively charged star polymer **18** could enter the live cells and serve as label agent [46]. Yin and co-workers [50] firstly reported an exciting application of **18** in

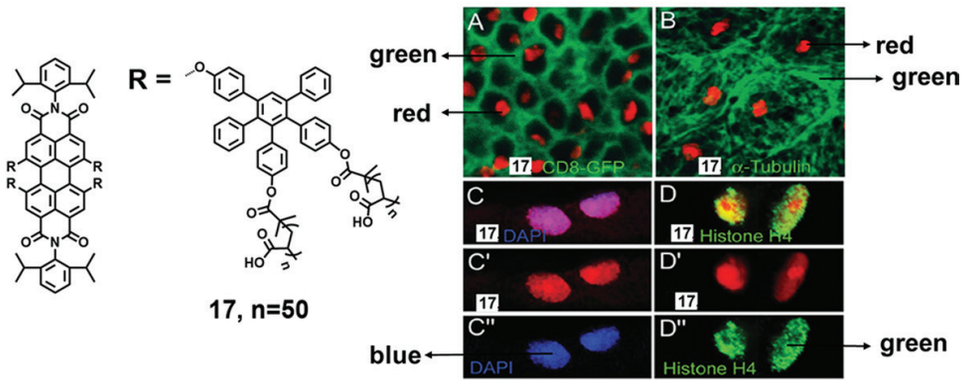

Figure 16. Chemical structure of **17** and Drosophila larval tissues observed by confocal microscopy. (A, green) Double staining of **17** (red) with CD8-GFP, (B, green) anti-α-tubulin. DAPI (blue, C-C″), and histone H4 (green, D-D″). C and D are combined channels while C′, C″ and D′, D″ are single channels. Copyright (2008), John Wiley and Sons.

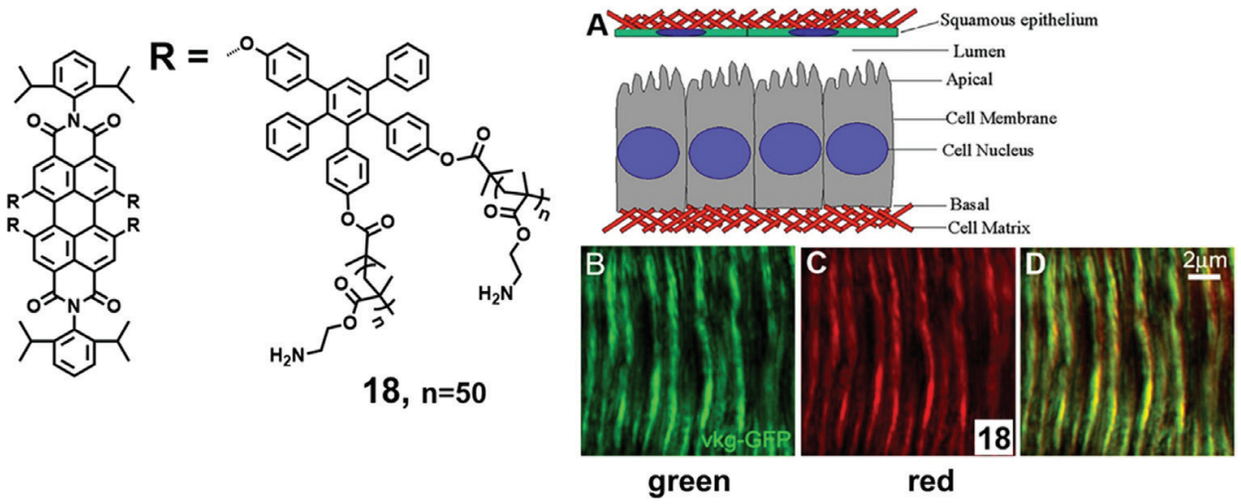

Figure 17. Chemical structure of **18** and illustration of extracellular matrix in a small central section of the Drosophila wing disc epithelium (A). ECM staining with Vkg-GFP (B, green) and **18b** (C, red) in living tracheal epithelium and merged channels (D). Copyright (2008), American Chemical Society.

2008, which could be used to directly mark the extracellular matrix network (**Figure 17A**) and visualize ECM network. The positively charged **18** could strongly bind with the negatively charged ECM components via electrostatic interactions in fixed or living tissue. **Figure 17** shows the high-resolution confocal microscopy image of ECM stained with **18** (red, **Figure 17C**) in living trachea epithelium. **18b** has the same specificity and much higher labelling speed compared with Vkg-GFP (green, **Figure 17D**). Besides, the fluorescence intensity of **18** increased remarkably after binding ECM, indicating the direct interaction between **18** and negatively charged ECM components. All the above results revealed that **18** could serve as ECM-labelling agent with high efficiency and specificity at the same time.

4. Conclusions and perspectives

This chapter gives a brief summary of the structures, self-assembly and biology applications of AIPDIs. AIPDIs have emerged as promising candidates for AIS and used in bio-applications. The synthetic strategies of AIPDIs are composed of the introduction of ionic substituents in the bay region, ortho or imide positions of PDIs. AIPDIs were found to form supramolecular-ordering construction by electrostatic interaction and other synergistic non-covalent interactions. By adjusting self-assembly conditions, AIPDIs have been successfully applied to form hierarchical organization in aqueous solution and bulk solid state. The biological applications involve studies *in vitro*, live cell and tissue imaging. Electrostatic interactions between AIPDIs and charged components in cells and tissues play an important role in these biological applications. To conclude, due to the high stability, water solubility, low cytotoxicity and desirable self-assembly behaviours, AIPDIs have great potential in biological applications and are still a topic of uninterrupted study.

Acknowledgements

This work was financially supported by the National Natural Science Foundation of China (21574009 and 51521062), Beijing Collaborative Innovative Research Center for Cardiovascular Diseases, and the Higher Education and High-quality and World-Class Universities (PY201605).

Author details

Meizhen Yin* and Baozhong Lü

*Address all correspondence to: yinmz@mail.buct.edu.cn

State Key Laboratory of Chemical Resource Engineering, Beijing Laboratory of Biomedical Materials, Beijing University of Chemical Technology, Beijing, China

References

[1] Motala-Timol S, Jhurry D, Zhou J, Bhaw-Luximon A, Mohun G, Ritter H. Amphiphilic poly(l-lysine-b-caprolactone) block copolymers: Synthesis, characterization, and solution properties. Macromolecules. 2008;**41**:5571-5576

[2] Chan S-C, Kuo S-W, Lu C-H, Lee H-F, Chang F-C. Syntheses and characterizations of the multiple morphologies formed by the self-assembly of the semicrystalline P4VP-b-PCL Diblock copolymers. Polymer. 2007;**48**:5059-5068

[3] Tung PH, Kuo SW, Chan SC, Hsu CH, Wang CF, Chang FC. Micellization and the surface hydrophobicity of amphiphilic poly(vinylphenol)-block-polystyrene block copolymers. Macromolecular Chemistry and Physics. 2007;**208**:1823-1831

[4] Colombani O, Ruppel M, Schubert F, Zettl H, Pergushov DV, Müller AH. Synthesis of poly(n-butyl acrylate)-block-poly(acrylic acid) diblock copolymers by ATRP and their micellization in water. Macromolecules. 2007;**40**:4338-4350

[5] Colombani O, Ruppel M, Burkhardt M, Drechsler M, Schumacher M, Gradzielski M, Schweins R, Müller AH. Structure of micelles of poly(n-butyl acrylate)-block-poly(acrylic acid) diblock copolymers in aqueous solution. Macromolecules. 2007;**40**:4351-4362

[6] Bhargava P, Tu Y, Zheng JX, Xiong H, Quirk RP, Cheng SZ. Temperature-induced reversible morphological changes of polystyrene-block-poly(ethylene oxide) micelles in solution. Journal of the. American Chemical Society. 2007;**129**:1113-1121

[7] Liu L, Gao X, Cong Y, Li B, Han Y. Multiple morphologies and their transformation of a polystyrene-block-poly(4-vinylpyridine) block copolymer. Macromolecular Rapid Communications. 2006;**27**:260-265

[8] Gohy J-F, Creutz S, Garcia M, Mahltig B, Stamm M, Jérôme R. Aggregates formed by amphoteric diblock copolymers in water. Macromolecules. 2000;**33**:6378-6387

[9] Du J, Chen Y. Organic-inorganic hybrid nanoparticles with a complex hollow structure. Angewendte Chemie International Edition. 2004;**43**:5084-5087

[10] Du J, Tang Y, Lewis AL, Armes SP. pH-sensitive vesicles based on a biocompatible zwitterionic diblock copolymer. Journal of the American Chemical Society. 2005; **127**:17982-17983

[11] Blanazs A, Madsen J, Battaglia G, Ryan AJ, Armes SP. Mechanistic insights for block copolymer morphologies: How do worms form vesicles? Journal of the American Chemical Society. 2011;**133**:16581-16587

[12] Yin M, Bauer R, Klapper M, Müllen K. Amphiphilic multicore-shell particles based on polyphenylene dendrimers. Macromolecular Chemistry and Physics. 2007;**208**:1646-1656

[13] Yin M, Cheng Y, Liu M, Gutmann JS, Müllen K. Nanostructured TiO_2 films templated by amphiphilic dendritic core-double-shell macromolecules: From isolated nanorings to continuous 2D mesoporous networks. Angewendte Chemie International Edition. 2008;**120**:8528-8531

[14] Discher DE, Eisenberg A. Polymer vesicles. Science. 2002;**297**:967-973

[15] Chen W, Meng F, Cheng R, Zhong Z. pH-Sensitive degradable polymersomes for triggered release of anticancer drugs: A comparative study with micelles. Journal of Controlled Release. 2010;**142**:40-46

[16] Yan Q, Zhou R, Fu C, Zhang H, Yin Y, Yuan J. CO_2-responsive polymeric vesicles that breathe. Angewendte Chemie International Edition. 2011;**123**:5025-5029

[17] Szostak JW, Bartel DP, Luisi PL. Synthesizing life. Nature. 2001;**409**:387-390

[18] Roodbeen R, van Hest J. Synthetic cells and organelles: Compartmentalization strategies. Bioessays. 2009;**31**:1299-1308

[19] Alpermann T, Rüdel K, Rüger R, Steiniger F, Nietzsche S, Filiz V, Förster S, Fahr A, Weigand W. Polymersomes containing iron sulfide (FeS) as primordial cell model: For the investigation of energy providing redox reactions. Origins of Life and Evolution of Biospheres. 2011;**41**:103-119

[20] Poulos TL. The Janus nature of heme. Natural Product Reports. 2007;**24**:504-510

[21] Wan X, Liu T, Liu S. Synthesis of amphiphilic tadpole-shaped linear-cyclic diblock copolymers via ring-opening polymerization directly initiating from cyclic precursors and their application as drug nanocarriers. Biomacromolecules. 2011;**12**:1146-1154

[22] Faul CFJ, Antonietti M. Ionic self-assembly: Facile synthesis of supramolecular materials. Advanced Materials. 2003;**15**:673-683

[23] Nakazono S, Imazaki Y, Yoo H, Yang J, Sasamori T, Tokitoh N, Cedric T, Kageyama H, Kim D, Shinokubo H. Regioselective Ru-catalyzed direct 2,5,8,11-alkylation of perylene bisimides. Chemistry—European Journal. 2009;**15**:7530-7533

[24] Ford WE. Photochemistry of 3,4,9,10-perylenetetracaboxylic dianhydride dyes: Visible absorption and fluorescence of di(glycyl)- imide derivative monomer and dimer in basic aqueous solutions. Journal of Photochemistry. 1987;**37**:189-204

[25] Schnurpfeil G. Syntheses of uncharged, positively and negatively charged 3,4,9,10-perylene-bis(dicarboximides). Dyes Pigmentation. 1995;**27**:339-350

[26] Sukul PK, Singh PK, Maji SK, Malik S. Aggregation induced chirality in a self-assembled perylene based hydrogel: Application of the intracellular pH measurement. Journal of Materials Chemistry B. 2013;**1**:153-156

[27] Deligeorgiev T, Zaneva D, Petkov I, Timcheva I, Sabnis R. Synthesis and properties of fluorescent bis-quaternized perylene dyes. Dyes Pigmentation. 1994;**24**:75-81

[28] Huang Y, Quan B, Wei Z, Liu G, Sun L. Self-assembled organic functional nanotubes and nanorods and their sensory properties. Journal of Physics and Chemistry C. 2009;**113**:3929-3933

[29] Guan Y, Yu S, Antonietti M, Bottcher C, Faul C. Synthesis of supramolecular polymers by ionic self-assembly of oppositely charged dyes. Chemistry—A European Journal. 2005;**11**:1305-1311

[30] Echue G, Lloyd G, Faul C. Chiral perylene diimides: Building blocks for ionic self-assembly. Chemistry—A European Journal. 2015;**21**:5118-5128

[31] Supur M, Fukuzumi S. Photodriven electron transport within the columnar perylenediimide nanostructures self-assembled with sulfonated porphyrins in water. Journal of Physics and Chemistry C. 2012;**116**:23274-23282

[32] Rao K, George S. Supramolecular alternate Co-assembly through a non-covalent amphiphilic design: Conducting nanotubes with a mixed D-A structure. Chemistry—A European Journal. 2012;**18**:14286-14291

[33] Weitzel C, Everett T, Higgins D. Aggregation and its influence on macroscopic in-plane organization in thin films of electrostatically self-assembled perylene-diimide/polyelectrolyte nanofibers. Langmuir. 2009;**25**:1188-1195

[34] Ma T, Li C, Shi G. Optically active supramolecular complex formed by ionic self-assembly of cationic perylenediimide derivative and adenosine triphosphate. Langmuir. 2008;**24:**43-48

[35] Zhang Z, Zhan C, Zhang X, Zhang, S, Huang J, Li A, Yao J. A self-assembly phase diagram from amphiphilic perylene diimides. Chemistry—A European Journal. 2012;**18**, 12305-12313

[36] Kainthan RK, Brooks DE. Unimolecular micelles based on hydrophobically derivatized hyperbranched polyglycerols: Biodistribution studies. Bioconjugate Chemistry. 2008;**19**:2231-2238

[37] He B, Chu Y, Yin M, Müllen K, An C, Shen J. Fluorescent nanoparticle delivered dsRNA toward genetic control of insect pests. Advanced Materials. 2013;**25**:4580-4584

[38] Yin M, Kang N, Cui G, Liu Z, Wang F, Yang W, Klapper M, Müllen K. Synthesis, electrochemical properties and self-assembly of a proton-conducting core-shell macromolecule. Chemistry—A European Journal. 2012;**18**:2239-2243

[39] Xu Z, He B, Wei W, Liu K, Yin M, Yang W, Shen J. Highly water-soluble perylenediimide-cored poly(amido amine) vector for efficient gene transfection. Journal of Materials Chemistry B. 2014;**2**:3079-3086

[40] Morgenroth F, Reuther E, Müllen K. Polyphenylen-dendrimere: von dreidimensionalen zu zweidimensionalen strukturen. Angewendte Chemie International Edition in England. 1997;**36**:631-634

[41] Liu X, He B, Xu Z, Yin M, Yang W, Zhang H, Cao J, Shen J. A functionalized fluorescent dendrimer as a pesticide nanocarrier: Application in pest control. Nanoscale. 2015;**7**:445-449

[42] You S, Cai Q, Müllen K, Yang W, Yin M. pH-sensitive unimolecular fluorescent polymeric micelles: From volume phase transition to optical response. Chemical Communication. 2014;**50**:823-825

[43] Yin M, Feng C, Shen J, Yu Y, Xu Z, Yang W, Knoll W, Müllen K. Dual-responsive interaction to detect DNA on template-based fluorescent nanotubes. Small. 2011;**7**:1629-1634

[44] Feng C, Yin M, Zhang D, Zhu S, Caminade AM, Majoral JP, Müllen K. Fluorescent core-shell star polymers based bioassays for ultrasensitive DNA detection by surface plasmon fluorescence spectroscopy. Macromolecular Rapid Communications. 2011;**32**:679-683

[45] Wang B, Yu C. Fluorescence turn-on detection of a protein through the reduced aggregation of a perylene probe. Angewendte Chemie International Edition. 2010;**49**:1485-1488

[46] You S, Cai Q, Zheng Y, He B, Shen J, Yang W, Yin M. Perylene-cored star-shaped polycations for fluorescent gene vectors and bioimaging. ACS Applied Materials Interfaces. 2014;**6**:16327-16334

[47] Xu Z, He B, Shen J, Yang W, Yin M. Fluorescent water-soluble perylenediimide-cored cationic dendrimers: Synthesis, optical properties, and cell uptake. Chemical Communications. 2013;**49**:3646-3648

[48] Yin M, Kuhlmann CR, Sorokina K, Li C, Mihov G, Pietrowski E, Koynov K, Klapper M, Luhmann HJ, Weil T. Novel fluorescent core–shell nanocontainers for cell membrane transport. Biomacromolecules. 2008;**9**:1381-1389

[49] Yin M, Shen J, Gropeanu R, Pflugfelder GO, Weil T, Müllen K. Fluorescent core/shell nanoparticles for specific cell-nucleus staining. Small. 2008;**4**:894-898

[50] Yin M, Shen J, Pflugfelder GO, Müllen K. A fluorescent core-shell dendritic macromolecule specifically stains the extracellular matrix. Journal of the American Chemical Society. 2008;**130**:7806-7807